EXTRACTING INFORMATION FROM SMITH-PURCELL FEL SIMULATIONS

J.T. Donohue, Centre d'Etudes Nucléaires de Bordeaux-Gradignan, BP 120, 33175 Gradignan, France
J. Gardelle, CEA CESTA, BP 2, F-33114 Le Barp, France

Abstract

Simulations of coherent Smith-Purcell radiation using 2D particle-in-cell codes have provided insight into the nature of the process, and have generally provided support to the viewpoint of the Vanderbilt University FEL group. However, if one is interested in terahertz frequencies, the need for small meshes and short time intervals makes the calculations exceedingly long. In particular, the S-P correlation between frequency and angle is only valid at distances large compared to the grating size, and may not be apparent if the simulation area is too small. With the help of the multipole expansion, we show how simulation data obtained with a small area may be extended to an area of arbitrary size. This enables us to confirm the presence of coherent higher order S-P peaks at the appropriate angles. We also isolate the forward and backward surface Floquet waves. Evidence for the presence of unsuspected components is presented.

INTRODUCTION

In attempting to simulate Smith-Purcell (S-P) radiation at terahertz frequencies with a 2D particle-in-cell code, one is confronted with problems of time and memory, at least if the simulation is performed on a PC. The reasons are easy to understand. Typical wavelengths are hundreds of μm, which means that mesh sizes must be tens of μm. The time step is tied to the mesh size Δ through stability conditions, and is, typically Δ/c, where c denotes the speed of light. Finally, the overall size of the simulation area is determined by the experimental circumstances. For example, the Dartmouth College experiment[1]using a low energy continuous electron beam has a grating about 12.7 mm long, and we perform our simulation in an area of approximately 20 mm $\times$ 5 mm, with Δ = 10 μm. To follow the system through one ns takes about 10 hours of calculation with the commercially available code we use, MAGIC[2]. In contrast the MIT experiment using a 15 MeV pre-bunched beam[3](at 17.1 GHz) had a grating 10 cm long, which means that our simulation area must be considerably larger than for the Dartmouth set-up. However, two ns are all that is needed to get a satisfactory simulation, since the beam is already bunched. At FEL 2005,[4]we reported our first attempts to simulate coherent S-P radiation in these two experiments. While we did find some interesting results, we used an unrealistically large current in the Dartmouth case, which led to copious emission of radiation from the ends of the grating at a frequency less than any allowed S-P frequency. This corresponded to the evanescent surface wave predicted by the theory of Andrews and Brau (AB)[5] but it obscured the true S-P signal that we sought. In the MIT simulation, we found that there remained a substantial emission of radiation even when we removed the grating. Furthermore, although we observed up to 20 harmonics of the bunching frequency, we didn't see the usual S-P relation between wavelength and angle. This is given by $\lambda = L(1/\beta - \cos\phi)/n$, where λ is the wavelength, L the grating period, β the relative velocity (in a plane parallel to the grating and perpendicular to the direction of the grooves), ϕ the angle of emission (with respect to the beam direction), and the integer n denotes the order. While this relation is true, it only holds precisely when the radiation is observed at distances large compared to both the wavelength and the grating size. Given the constraints of small mesh size, it is impractical to simulate in an area large enough to see the wavelength-angle correlation.

Another problem we encountered was the presence on the grating surface of two distinct surface waves. One of these, according to the AB theory, is in resonance with the electron beam, while the other, of the same frequency but propagating in the opposite direction, is generated by reflection at the grating ends. It is of some interest to isolate these two Floquet waves, in order to obtain a direct verification of the AB theory, and to determine the reflection coefficient when such a wave reaches the grating end. This coefficient may be used in a refinement of the AB theory proposed by Andrew, Boulware, Brau and Jarvis[6]in order to estimate the start current needed to produce coherent S-P radiation in the Dartmouth experiment. In reference 6 an estimate of 50 A/m was made, while Kumar and Kwang-Je Kim[7] obtained a slightly smaller value of 36.5 A/m.

In this paper we describe two methods we have developed to address these problems. The first method we call the Small Box→Big Box transformation, since it allows us to simulate in a small area and extrapolate to a much larger area, so as to see the S-P wavelength-angle correlation. While the near-to-far-field transformation is the subject of a chapter of Taflove's monograph[8],our simple method uses Finite Fourier Transforms (FFT) and fitting procedures readily available in such high-level programs as *Mathematica* and MAPLE, and thus involves relatively little effort on the part of the user. The second

method has been developed to extract from a simulation the two oppositely moving Floquet evanescent waves, which are important only in the neighborhood of the grating. Again, the FFT and fitting capacities of *Mathematica* or MAPLE may be used to execute the task.

In Section II we describe the Small Box→Big Box transformation as applied to a MIT simulation. In Section III we show how to separate the Floquet components from a simulation of the Dartmouth set-up. The anomalies observed in our fitting procedure reveal an unsuspected presence of higher temporal harmonics in the field, as well as incipient coherent S-P radiation. Our conclusions are given in Section IV.

SMALL BOX→BIG BOX TRANSFORMATION

In a source-free half-plane region extending to infinity, the magnetic field in the z-direction may be written as

$$B_z(\rho,\phi,t)=\Re\int_0^\infty d\omega e^{-i\omega t}\sum_{m=1}^{\infty}\sin(m\phi)H_m^1\left(\frac{\omega\rho}{c}\right)b_m(\omega),$$

where the standard Hankel functions H_m^1 are used and the complex quantities $b_m(\omega)$ are the coefficients of the multipole field. They may be written as

$$b_m(\omega)=\frac{2}{\pi^2 H_m^1\left(\frac{\omega\rho_0}{c}\right)}\int_{-\infty}^{\infty}dt e^{i\omega t}\int_0^\pi d\phi\sin(m\phi)B_z(\rho_0,\phi,t).$$

The azimuthal component of the electric field (cgs units) may then be written as

$$E_\phi(\rho,\phi,t)=-\Re\int_0^\infty d\omega e^{-i\omega t}\sum_{m=1}^{\infty}i\sin(m\phi)H_m^{1\prime}\left(\frac{\omega\rho}{c}\right)b_m(\omega)$$

The total energy/cm radiated across a semicircle of radius ρ is then

$$\frac{dW}{dz}=\left(\frac{c\rho}{4\pi}\right)\int_{-\infty}^{\infty}dtE_\phi(\rho,\phi,t)B_z(\rho,\phi,t)$$

which reduces, after some manipulations involving the Wronskian, to

$$\frac{dW}{dz}=\frac{c^2}{4}\int_0^\infty d\omega\sum_{m=1}^{\infty}\frac{|b_m(\omega)|^2}{\omega},$$

which is independent of the radius.

In the context of our simulation, we calculate $B_z(\rho_0,\phi_k,t_r)$, with $\phi_k=(2k-1)\pi/180,\ 1\le k\le 90$ and $t_r=t_1+(r-1)T/N,\ 1\le r\le N$, where the time step T/N is chosen by MAGIC. Accordingly, we use FFT rather than continuous Fourier transforms, and we perform a FFT at each of the 90 angles, obtaining $\tilde{b}(s,\phi_k)=\mathrm{FFT}(B_z(\rho_0,\phi_k,t_r))$, where $\omega\to 2\pi(s-1)/T$. Then at fixed s, we write

$$\tilde{b}(s,\phi_k)=\sum_{m=1}^{85}\tilde{b}_m(s)\sin(m\phi_k)$$

and we apply a fitting procedure to determine the $\tilde{b}_m(s)$ for $1\le m\le 85$. Finally we introduce the normalized multipole coefficients $\hat{b}_m(s)$,

$$\hat{b}_m(s)=\tilde{b}_m(s)/H_m^1(2\pi(s-1)\rho_0/cT).$$

We may now calculate the magnetic field and the azimuthal component of the electric field at any point in the source-free region by taking the Inverse FFT of the sequence of sums

$$B_z(\rho,\phi,t)=\mathrm{IFFT}(\left\{\sum_{m=1}^{85}\hat{b}_m(s)\sin(m\phi)H_m^1(2\pi(s-1)\rho/cT)\right\})$$

$$E_\phi(\rho,\phi,t)=\mathrm{IFFT}(\left\{\sum_{m=1}^{85}-i\hat{b}_m(s)\sin(m\phi)H_m^{1\prime}(2\pi(s-1)\rho/cT)\right\})$$

It is often desirable to examine the fields in a given frequency range, and this may be accomplished by introducing a filter in the Inverse FFT. We should point out that since the FFT assumes a periodic function, the time behavior we obtain at an arbitrary point may violate causality. However, an *ad hoc* translation in time allows one to find the true pulse shape at the new radius.

The energy radiated during the interval of time T is given by (ergs/cm if $\hat{b}_m(s)$ is in Gauss)

$$\frac{dW}{dz}=\left(\frac{c^2T^2}{4\pi^2N}\right)\sum_{s=2}^{N}\left(\left(\sum_{m=1}^{85}|\hat{b}_m(s)|^2\right)/(s-1)\right).$$

To illustrate this procedure, we plot in Figure (1) our simulated $B_z(t)$ (for the MIT set-up) *vs.* t at a distance 5.5 cm from the center of the grating, and at angle 89°, with its FFT.

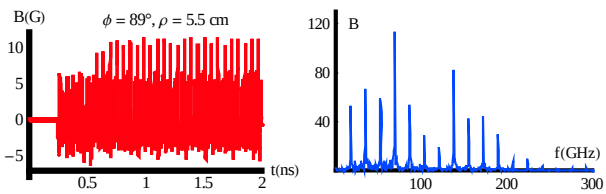

Figure 1. $B_z(t)$ *vs.* t and its FFT, ϕ = 89°, ρ = 5.5cm.

After performing the operations indicated above, we obtain the extrapolated function $B_z(t)$ *vs.* t at a distance 50 cm from the center, again with its FFT, which are shown in Figure (2).

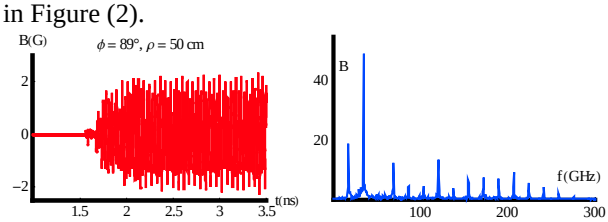

Figure 2. $B_z(t)$ *vs.* t and its FFT, ϕ = 89°, ρ = 50 cm.

The reconstructed signal is smaller than the original, as expected, since the fields decrease asymptotically as $\rho^{-1/2}$. Even taking into account the overall reduction in size, the reconstructed FFT is quite different from that at small radius. This must be attributed to the fact that for the

second harmonic, there is a broad S-P first order peak at 82°, close enough to our angle of 89° to favor the frequency near 34 GHz.

To indicate how the small box → big box transformation affects the angular distribution of energy, we show in Figure (3) the energy radiated during our 2 ns pulse as a function of angle for a band of frequencies centered around the sixth harmonic, near 103 GHz.

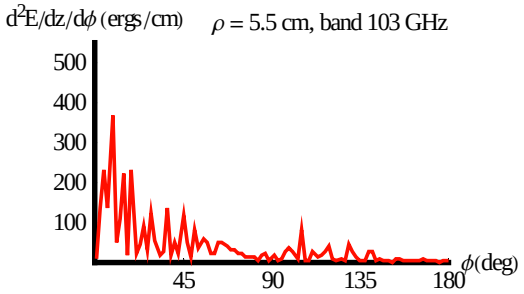

Figure 3. The angular distribution of energy at 5.5 cm in a frequency band centered at 103 GHz.

For comparison we show in Figure (4) the reconstructed distribution of energy as predicted by our small box → big box transformation with ρ = 50 cm. The angles at which coherent S-P radiation is expected in the MIT experiment at this frequency are indicated. For both distributions we find the same total energy radiated

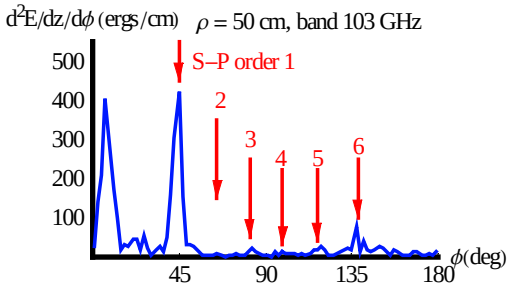

Figure 4. The reconstructed angular distribution of energy at 50 cm in a frequency band centered at 103 GHz.

119.3 ergs/cm, calculated by numerical integration. This in good agreement with the direct formula for the energy radiated in that band. Results similar to these were obtained for the first 20 harmonics. The prominent peak at small angles (8° here) is not S-P radiation but is associated with the appearance and disappearance of short current pulses, even in the absence of a grating.

ISOLATING FLOQUET WAVES

In the AB approach the electron beam interacts with a component of an evanescent Floquet wave. In the Dartmouth configuration, the wave has a negative group velocity, and the mechanism is that of a Backward Wave Oscillator. Upon reaching the end of the grating, the wave is partly reflected, and some of its energy is emitted as free radiation. The magnetic field in the neighborhood of the grating is then a sum of two Floquet evanescent waves propagating in opposite directions, and one may write,

$$B_z(x,y,t) = \Re \sum_{p=-\infty}^{\infty} e^{-\alpha_p y}\left\{B_p e^{i((k_F+pK)x-\omega t)} + B'_p e^{i((-k_F-pK)x-\omega t)}\right\}$$

where $\alpha_p = \sqrt{(k_F + pK)^2 + (\omega/c)^2}$.

The reflected wave is not in resonance with the beam, and essentially traverses the grating without change, until it is also reflected at the other end, again emitting radiation. To better understand this, we have developed a simple method for isolating the Floquet waves. We use the "range" command of MAGIC, which measures a component of the electromagnetic field along some straight line in space (along the *x*-direction here), at a fixed time. An example is shown in Figure (5).

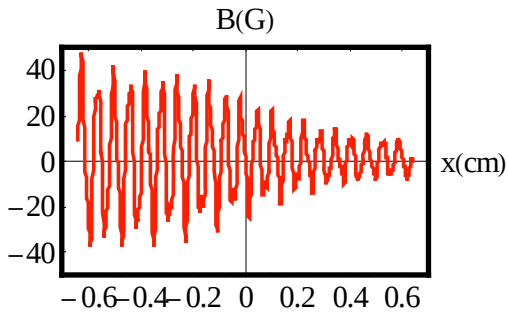

Figure 5. B_z *vs. x* at fixed *t* and *y*. Dartmouth Grating.

By performing three ranges separated by short time intervals, obtaining the spatial FFTs and fitting the three complex amplitudes for each wave number *k* to an assumed form $\alpha_k e^{-i\omega t} + \beta_k e^{i\omega t}$, we can empirically determine the coefficients α_k and β_k. An FFT is shown in

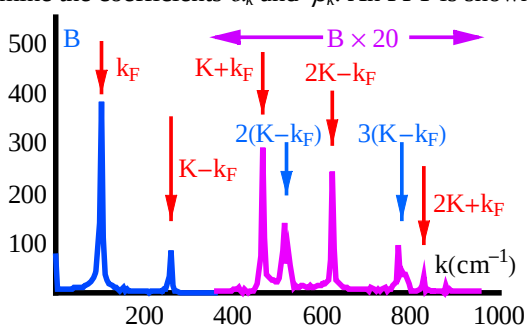

Figure 6. FFT of signal in Figure 5.

Figure (6). The prominent peaks are indicated by red arrows, and the right-hand side of the figure has been multiplied by 20 to make details visible. The blue arrows indicate second and third harmonics of K-k_F, the component resonant with the beam. Here the frequency ω is known ($2\pi f$, with f = 432 GHz). By comparing with the general expression for B_z, we see that the components of the Forward Floquet wave have peaks at $k_F + pK$, while the Backward Floquet wave has support at pK-k_F. If we multiply the α_k by a filter that includes only the peaks at $k_F + pK$, and perform the Inverse FFT, we obtain the

Forward Floquet waves at each of the three instants. Similarly, by filtering around pK-k_F, we find the backward wave, and both are shown in Figure (7).

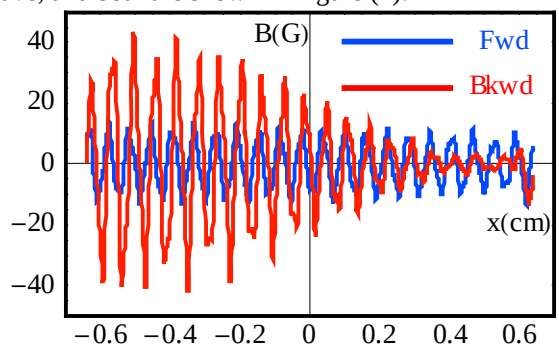

Figure 7. Forward (blue) and backward (red) Floquet waves extracted from signal in Figure 5.

It is clear from this figure that the forward Floquet wave shows little or no growth across the grating, while the backward wave shows considerable growth, indicating an imaginary part of k of order 4 cm^{-1}. We note also that at both ends of the grating the ratio of the incident to the reflected wave is approximately 3:1.

As a check on our empirical method, which uses a least-square method to fit all the FFT components, we attempted to see whether the fit is adequate. This led to a somewhat serendipitous discovery that we now discuss. If we define

$$\Delta B_k(t) = \mathrm{FFT}_k(t) - \alpha_k e^{-i\omega t} - \beta_k e^{i\omega t},$$

the complex number that is a measure of the validity of our fit, we may plot its absolute value as a function of wave number. The results are shown in Figure (8). The

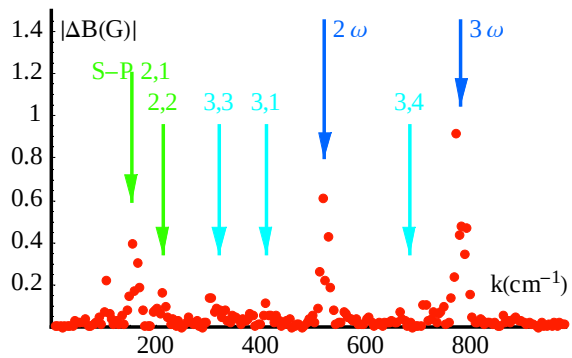

Figure 8. Discrepancy ΔB *vs.* wave number k.

major anomalies occur at 520 and 780 cm^{-1}, which are just the second and third harmonics, respectively, of the resonant wave number, 260 cm^{-1}. They appear also in Figure (6). Upon examining the data, we found that these anomalies disappear if we fit using 2ω and 3ω instead of ω in our fitting procedure. That means that there are components of the form $e^{im((K-k_F)x-\omega t)}$, with m = 2, 3, etc. Such components are readily found in the FFT analysis of the current, and they follow from the non-linear nature of the bunching phenomenon. By an argument based on Ampère's law, modulation of the current must appear as modulation in the magnetic field, and that is what we see. Aside from these two major anomalies, there appear to be several smaller ones. We attribute these to the presence, in small amounts, of the coherent S-P signal corresponding to various harmonics and orders. From the S-P relation and the fact that all coherent radiation will occur at a multiple of the frequency of the evanescent wave, one may derive the following expression,

$$k = m\omega/\beta c - 2\pi n/L,$$

where n denotes the order, m the harmonic, the period L is 173 μm, and $\omega = 2\pi \times 4.32\times10^{11}$ s^{-1}. Using it we have drawn arrows to indicate the wave numbers associated with some pairs m, n. It must be noted that our FFT is symmetric, and peaks that should occur for negative k values are shown at positive values.

CONCLUSIONS

We have presented results concerning our attempts to extract information from simulations of coherent Smith-Purcell Radiation, using a 2-D PIC code. Two distinct methods have been discussed. One permits results obtained in a small area to be extended to a larger area. In doing so, we see more clearly the coherent S-P radiation produced in the MIT experiment with a high-energy pre-bunched beam. The second method involves fitting the FFT data at three closely spaced times, in order to separate the forward and backward Floquet surface waves postulated in the approach of Andrews and Brau. As a by-product, the presence of second and third harmonics of the fundamental bunching component were demonstrated, and evidence for tiny amounts of coherent S-P radiation was provided.

REFERENCES

[1] A. Bakhtyari, J. E. Walsh, and J. H. Brownell, Phys. Rev. E **65**, 066503 (2002).
[2] MAGIC, Mission Research Corporation.
[3] S.E. Corbly, A. S. Kesar, J. R. Sirigiri, and R. J. Temkin, Phys. Rev. Lett. **94**, 054803 (2005).
[4] JT. Donohue and J. Gardelle, *Proceedings of the 2005 FEL Conference, Stanford,California USA* p. 262 (http://www.JACoW.org).
[5] H.L. Andrews and C.A. Brau, Phys. Rev. ST Accel. Beams **7**, 070701 (2004).
[6] H.L.Andrews, C. H. Boulware, C. A. Brau and J. D. Jarvis, , Phys. Rev. ST Accel. Beams **8**, 050703 (2005).
[7] Vinit Kumar and Kwang-Je Kim, Phys. Rev. E **73**, 026501 (2006).
[8] A.Taflove, *Computational Electrodynamics*, (Artech House, Boston, 1995), p. 203.